

# Manganese-Enhanced MRI of Mouse Heart During Changes in Inotropy

Tom C.-C. Hu,<sup>1,3</sup> Robia G. Pautler,<sup>5</sup> Guy A. MacGowan,<sup>4</sup> and Alan P. Koretsky<sup>1,2\*</sup>

**Recently the dual properties of manganese ion ( $Mn^{2+}$ ) as an MRI contrast agent and a calcium analogue to enter excitable cells has been used to mark specific cells in brain and as a potential intracellular cardiac contrast agent. Here the hypothesis that in vivo manganese-enhanced MRI (MEMRI) can detect changes in inotropy in the mouse heart has been tested.  $T_1$ -weighted images were acquired every minute during an experimental time course of 75 min. Varying doses of  $Mn^{2+}$  (3.3–14.0 nmoles/min/g BW) were infused during control and altered inotropy with dobutamine (positive inotropy due to increased calcium influx) and the calcium channel blocker diltiazem (negative inotropy). Infusion of  $MnCl_2$  led to a significant increase in signal enhancement in mouse heart that saturated above  $3.3 \pm 0.1$  nmoles/min/g BW  $Mn^{2+}$  infusion. At the highest  $Mn^{2+}$  dose infused there was a 41–47% increase in signal intensity with no alteration in cardiac function as measured by MRI-determined ejection fractions. Dobutamine increased both the steady-state level of enhancement and the rate of MRI signal enhancement. Diltiazem decreased both the steady-state level of enhancement and the rate of MRI signal enhancement. These results are consistent with the model that  $Mn^{2+}$ -induced enhancement of cardiac signal is indicative of the rate of calcium influx into the heart. Thus, the simultaneous measurement of global function and calcium influx using MEMRI may provide a useful method of evaluating in vivo responses to inotropic therapy. Magn Reson Med 46:884–890, 2001. Published 2001 Wiley-Liss, Inc.<sup>†</sup>**

**Key words:** calcium influx; cardiac MRI; dobutamine; diltiazem; imaging inotropy

There has been rapid development in functional cardiac MRI techniques. MRI can be used to assess anatomy as a function of cardiac cycle (1), regional blood flow using contrast agents (2) or endogenous arterial spin labeling techniques (3), and regional wall motion using phase-sensitive (4,5) or tagging techniques (6). In addition to MRI, spectroscopic techniques, including  $^{31}P$ ,  $^{13}C$ , and  $^{23}Na$ , offer a means to measure metabolic changes associated with changes in cardiac function (7). Intracellular calcium is a key regulator of myocardial contraction; however, there are few ways to assess this important factor. Fluorescent techniques have been widely used in isolated

cardiac myocytes, but these techniques cannot be extended to in vivo studies. MRI calcium probes, such as fluoroBapta and DOPTA-Gd, have not found widespread use (8,9).

One possible technique for assessing intracellular calcium is to use a paramagnetic agent that has physical properties similar to calcium, such as manganese ion ( $Mn^{2+}$ ).  $Mn^{2+}$  has an ionic radius similar to that of  $Ca^{2+}$ , and is handled similarly in many biological systems (10). For example,  $Mn^{2+}$  is known to enter cardiac myocytes through voltage-gated calcium channels (11,12).  $Mn^{2+}$  is also an excellent  $T_1$  contrast agent (13,14), and it was used as the first MRI contrast agent by Lauterbur and coworkers (15). These properties of  $Mn^{2+}$  (that it is an excellent MRI contrast agent and enters excitable cells like calcium) were recently used to detect active regions of the brain (16). In addition,  $Mn^{2+}$  was shown to be useful in tracing neuronal connections (17). This ability of  $Mn^{2+}$  to visualize cell activity on MRI indicates that  $Mn^{2+}$  might be a useful MRI agent for quantitating relative rates of calcium influx in the heart.

The fact that  $Mn^{2+}$  primarily enters cardiac cells through voltage-gated calcium channels predicts that the rate of influx into the heart should be altered under conditions that increase or decrease calcium influx into heart.  $\beta$ -Adrenergic agents, such as dobutamine, are known to increase calcium influx into the heart to increase contractile function. Calcium channel blockers, such as diltiazem, are known to decrease cardiac function by decreasing calcium influx into the heart. In this study we investigated the usefulness of  $Mn^{2+}$  as a measure of calcium influx and inotropic state in the heart by testing whether dobutamine increases and diltiazem decreases MRI enhancement during infusion of  $MnCl_2$ . In vivo experiments were performed on mouse heart using  $T_1$ -weighted fast low angle shot (FLASH) images under control and dobutamine- and diltiazem-induced changes in inotropy. Dobutamine increases the rate of signal enhancement and the steady-state level of enhancement, and diltiazem decreases the rate of enhancement and the steady-state level of enhancement obtained compared to controls. This occurred without any evidence for cardiotoxic effects of  $Mn^{2+}$  at the doses used. These data support the use of manganese-enhanced MRI (MEMRI) as a measure of calcium influx and cardiac inotropic state in the heart.

## MATERIALS AND METHODS

### Animal Preparation

Male FVB mice were used for all experiments. Avertin (2,2,2-tribromoethanol) was administered intraperitoneally at a dose of 0.017 ml/g body weight (BW) to initially anesthetize the mice. It was made from 0.5 ml of a stock

<sup>1</sup>Pittsburgh NMR Center for Biomedical Research, Carnegie Mellon University, Pittsburgh, Pennsylvania.

<sup>2</sup>Laboratory of Functional and Molecular Imaging, NINDS, NIH, Bethesda, Maryland.

<sup>3</sup>Department of Chemistry, Carnegie Mellon University, Pittsburgh, Pennsylvania.

<sup>4</sup>Cardiovascular Institute of the University of Pittsburgh Medical Center, Pittsburgh, Pennsylvania.

<sup>5</sup>Biological Imaging Center, Beckman Institute, California Institute of Technology, Pasadena, California.

Grant sponsor: NIH; Grant numbers: HL40354; HL03826.

\*Correspondence to: Alan P. Koretsky, Ph.D., In Vivo NMR Research Center, NINDS, NIH, 10 Center Drive, Room B1D-69B, MSC 1060, 9000 Rockville Pike, Bethesda, MD 20892. E-mail: koretskya@ninds.nih.gov

Received 18 January 2001; revised 18 April 2001; accepted 15 May 2001.

Published 2001 Wiley-Liss, Inc. <sup>†</sup> This article is a US Government work and, as such, is in the public domain in the United States of America.

solution (25 g avertin/15.5 ml T-amyl alcohol) that was diluted with 39.5 ml of distilled water. Anesthesia was maintained with 7  $\mu\text{l/g}$  BW avertin injected every 30–40 min via an i.p. line. This protocol was established to maintain a relatively constant level of anesthesia and heart rate during the MRI experiment. Once mice were anesthetized, an intravenous tail catheter was introduced, secured with suture ties, and connected directly to a syringe pump (Cole Palmer) to infuse  $\text{MnCl}_2$ .

## MRI

Images were acquired on a 7-T, 15-cm horizontal bore Bruker Avance spectrometer (Bruker Instruments, Billerica, MA) equipped with a 4.3-cm microimaging gradient insert. Procedures were as previously described (18). An in-house-built single-loop transmit/receive RF coil (diameter = 25 mm), tuned to the  $^1\text{H}$  frequency (300 MHz), was used to detect the signal to increase resolution and signal-to-noise ratio. The ECG signals were obtained with copper wires from the front paws of the animal with an electrical conducting gel to aid contact. This signal was preamplified and connected to a Gould universal amplifier (Gould Instrument Systems, Valley View, OH). The ECG signals were used to trigger the FLASH acquisition sequence (19). For experiments measuring ejection fraction, both ECG and respiratory gating were used. The respiratory signal was acquired through a water-filled balloon connected to a pressure transducer (Ohmeda DTX Plus disposable pressure transducer; Cardio Medical Products Inc., Rockaway, NJ) via PE-50 tubing. The balloon was placed on the side of the abdomen, and the respiratory signal was amplified with a Gould universal amplifier.

A pilot coronal image using an ECG-gated FLASH sequence was obtained, from which the long axis of the heart was identified. Single-slice, short-axis heart images were acquired with the cardiac-gated FLASH imaging sequence midway through the left ventricle and perpendicular to the long axis of the heart. Since the cardiac cycle was too fast for short-axis images to be acquired in one scan, 16 segments were used so that each segment contained four phase-encodes. The imaging parameters were as follows: matrix =  $128 \times 64$ ; TE = 1.3 ms; TR  $\approx$  300 ms; four phase-encodes/segment; slice thickness = 1.00 mm; FOV = 2.5 cm (except for ejection fraction measurements in which the FOV was 2 cm); and eight averages. Images acquired directly after the ECG gating of the R wave were assumed to be at end-diastole, as previously demonstrated (18). Image intensities in the relevant regions of interest (ROIs) were normalized to an external water phantom placed on the side of the mouse. Images were taken every minute to monitor signal changes over the course of an experiment. For all protocols, five to eight control images were taken prior to any infusion, and the average intensities of these control images were used to normalize individual time courses. Percent enhancements were calculated from the control intensities and the average values after steady state was achieved. To verify that signal intensity changes detected were not due to slight variations in TR due to variations in heart rate, a range of TRs from 300 ms to 700 ms were tested. The change in signal intensities due to the TR change was small compared to the

changes detected with  $\text{MnCl}_2$  under the imaging conditions used, and the percent enhancements were not significantly different (data not shown).

For functional analysis of the heart pre- and post- $\text{Mn}^{2+}$  infusion, the left ventricular ejection fraction was measured using MRI. Five FVB mice were used for MRI measurement of the left ventricular ejection fraction as a measure of cardiac function analysis pre- and post- $\text{Mn}^{2+}$  infusion at a dose of  $14.0 \pm 1.1$  nmoles/min/g BW ( $119.64 \pm 0.05$  mM  $\text{Mn}^{2+}$  infusion dose). By using various delay times between the MRI signal acquisitions and the ECG trigger pulse, a full cardiac cycle from single-slice images could be acquired. Percentage of cardiac cycle for each image acquisition was calculated using the ECG delay (manually set) normalized to the recorded measurement from the ECG. ROIs were used for left ventricular cavity area tracing (ParaVision software) and normalized to the average area obtained from the end-diastolic images.

## $\text{MnCl}_2$ Administration

### $\text{Mn}^{2+}$ Infusion Protocol

Three doses of  $\text{MnCl}_2$  were used:  $3.3 \pm 0.1$  nmoles/min/g BW,  $7.0 \pm 0.4$  nmoles/min/g BW, and  $14.0 \pm 1.1$  nmoles/min/g BW were infused into the mice via the tail vein line at a constant rate of 0.2 ml/h with the aid of a syringe pump (Cole Palmer). Three concentrations of  $\text{MnCl}_2$  solution were used to achieve these concentrations:  $29.99 \pm 0.03$  mM,  $60.08 \pm 0.00$  mM, and  $119.64 \pm 0.05$  mM. The appropriate amount of  $\text{MnCl}_2$  was dissolved in saline. For control, an iso-equivalent amount of NaCl comparable to  $14.0 \pm 1.1$  nmoles/min/g BW  $\text{MnCl}_2$  solution was added to saline and infused at the same rate as the  $\text{MnCl}_2$ . The total infusion time was 30 min, using a total volume of 0.1 ml. Due to the slow infusion rates and the animal-to-animal variation in the volume of the saline solution in the i.v. line, the time when the  $\text{Mn}^{2+}$  solution entered the mouse circulation was variable. To normalize this variation, the time courses of signal intensity changes were aligned to each half-maximal signal intensity change point.

### Altering Cardiac Inotropy

Dobutamine (1.5  $\mu\text{g/g}$  BW i.p.) was administered to cause positive inotropy and an increase in myocyte  $\text{Ca}^{2+}$  influx (20). The onset of the dobutamine effect was monitored by the heart rate increase, and lasted for 12–15 min. The effects of dobutamine on MRI signal enhancement due to  $\text{MnCl}_2$  infusion were examined with two  $\text{MnCl}_2$  doses of 14.0 nmoles/min/g BW ( $N = 4$ ) and 3.3 nmoles/min/g BW ( $N = 2$ ).

Diltiazem (0.016 mg/min/g BW, iv) was used to induce negative inotropy by blocking calcium channels (21). As there were no significant signal intensity enhancement differences between the two doses of  $\text{Mn}^{2+}$  used in the dobutamine experiments, the diltiazem was used with the lower  $\text{Mn}^{2+}$  dose (3.3 nmoles/min/g BW;  $N = 5$ ).

### Statistics

Unless otherwise stated, the differences between different manganese groups of mice were assessed using ANOVA with a Scheffe's test. Values reported are mean  $\pm$  SD.

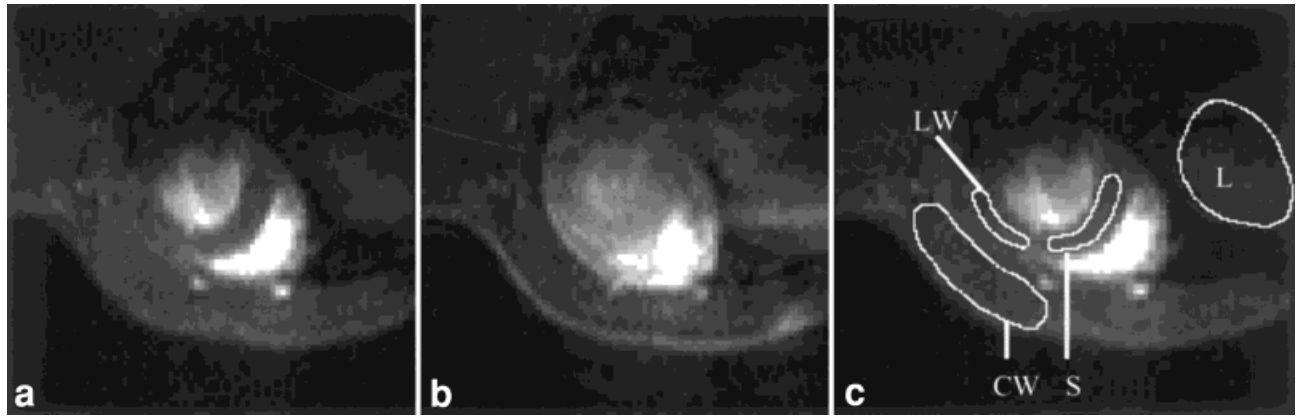


FIG. 1. Examples of short-axis images from the heart of an FVB mouse before and after  $Mn^{2+}$  infusion: (a) image obtained prior to  $Mn^{2+}$  infusion, and (b) image obtained after 30 min of 14.0 nmoles/min/g BW  $Mn^{2+}$  infusion. c: Image of the heart showing the ROIs that were used for signal intensity analysis. These included the S, LW, L, and CW.

**RESULTS**

Infusion of  $Mn^{2+}$  via the mouse tail vein leads to significant signal enhancement in  $T_1$ -weighted images. Figure 1 shows the  $T_1$ -weighted short-axis heart images of an FVB mouse infused with  $MnCl_2$  solution. Figure 1a shows the pre- $Mn^{2+}$  infusion image, and Fig. 1b shows the post- $Mn^{2+}$  infusion image. The signal intensity enhancement is clearly seen. ROIs for the interventricular septum (S), left ventricular free wall (LW), liver (L), and chest wall (CW) were used for signal intensity analysis (Fig. 1c). Time courses of  $T_1$ -weighted MRI signal intensity changes in the LW are shown in Fig. 2.  $Mn^{2+}$  infusion leads to an approximately 40–50% increase in signal in normal hearts. The figure shows the signal enhancement changes during the whole experimental course, in which images were taken every minute starting from the pre- $Mn^{2+}$  enhancement control images. In the control experiments shown in Fig. 2 (open diamond), the solution contains NaCl in addition to the saline solution in order to match the osmolarity of the 119.64 mM  $Mn^{2+}$  solution. In the  $Mn^{2+}$  infusion experiment shown in Fig. 2 (filled squares), each point rep-

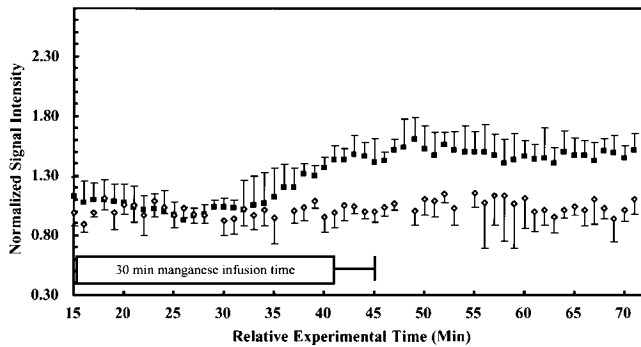


FIG. 2. Time course of  $T_1$ -weighted MRI signal intensity changes in the LW for control (open diamond), and 14.0 nmoles/min/g BW infusion of  $Mn^{2+}$  (filled square). Each point represents the average pixel value taken from the left ventricular ROI and normalized to an external reference of distilled water and the average of five to eight control images taken before starting the infusion. (Error bars = 1 SD.)

resents the average pixel value taken from the ROI (LW in this case) and normalized to both an external reference (distilled water) and the average of the control images taken pre- $Mn^{2+}$  infusion.

Left ventricular ejection fraction was measured pre- and post- $Mn^{2+}$  to determine if  $Mn^{2+}$  infusion at the doses used affects cardiac function. Figure 3a shows one normalized cardiac cycle for pre- $Mn^{2+}$  infusion, and Fig. 3b shows one

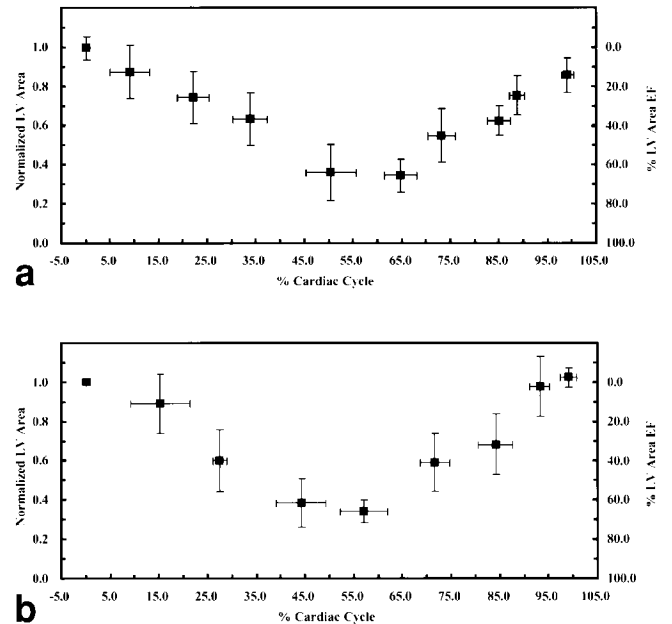


FIG. 3. Functional analysis of the mouse heart before and after 14.0 nmoles/min/g BW  $Mn^{2+}$  infusion. a: Normalized cardiac cycle for hearts prior to  $Mn^{2+}$  infusion ( $N = 5$ ). b: Normalized cardiac cycle for hearts after  $Mn^{2+}$  infusion ( $N = 5$ ). The x-axis represents the percent cardiac cycle for each image acquisition calculated by using the ECG delay normalized to the recorded heart rate. The y-axis represents the area of the left ventricle normalized to the average of end-diastolic area and the estimated ejection fraction from the normalized left ventricular area. There were no significant differences in diastolic left ventricular areas or ejection fraction before and after  $Mn^{2+}$  infusion. (Error bars = 1 SD.)

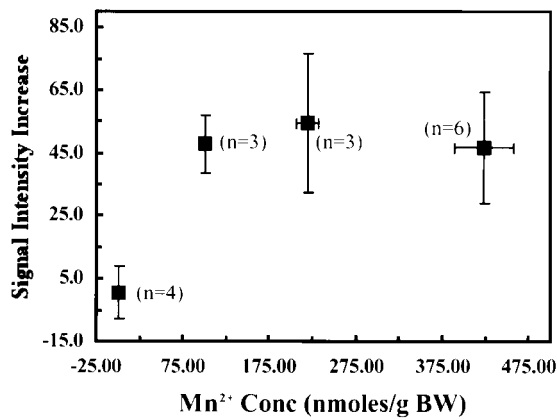


FIG. 4. Effect of altering the concentration of infused  $\text{Mn}^{2+}$  on  $T_1$ -weighted signal enhancement from the LW. The x-axis shows the total concentration of onset infused  $\text{Mn}^{2+}$  normalized to mouse BW. The y-axis shows the signal intensity changes in percent after the signal intensity plateaued, normalized to the preinfusion signal. (Error bars = 1 SD.)

normalized cardiac cycle for post- $\text{Mn}^{2+}$  infusion at a dose of 14.0 nmoles/min/g BW. The x-axis represents the percent cardiac cycle for each image acquisition calculated by using the ECG delay (manually set) normalized to the HR recorded from the ECG. The y-axis represents the relative left ventricular area normalized to the average of end-diastolic image(s). There was no significant difference in LV end-diastolic areas pre- ( $0.093 \pm 0.023 \text{ cm}^2$ ) and post- ( $0.087 \pm 0.006 \text{ cm}^2$ )  $\text{Mn}^{2+}$  infusion (with  $P = 0.6255$ ;  $N = 5$ ). The ejection fraction is approximately 65–66% for both pre- and post- $\text{Mn}^{2+}$  infusion from the single-slice, short-axis heart images. Therefore, manganese infusion in the

range of 3.3–14.0 nmoles/min/g BW does not depress cardiac function from single-slice LV open-area ejection fraction estimates in the mouse. In addition, there was no significant change in HR pre- and post- $\text{Mn}^{2+}$  infusion ( $368 \pm 30$  and  $377 \pm 40$  BPM, respectively).

The dose dependence of the steady-state signal enhancement detected after 30 min infusion of various doses of  $\text{MnCl}_2$  is shown in Fig. 4. Left ventricular signal intensities were acquired from ROIs as shown in Fig. 1 and normalized to pre- $\text{Mn}^{2+}$  infusion controls. The signal enhancement reaches a plateau at an infused  $\text{Mn}^{2+}$  dose of 3.3 nmoles/min/g BW. Table 1 shows all the numerical results from all the ROIs collected. For S, the signal enhancement range is 41–46%, after which it plateaus. For LV, values are 47–55%. For CW and L, enhancements reach 2–19% and 40–67%, respectively.

To test whether alterations in cardiac inotropy affect the MRI signal enhancements detected with  $\text{Mn}^{2+}$  infusion, dobutamine (increased calcium influx) or diltiazem (decreased calcium influx) were used. The time courses of  $T_1$ -weighted MRI signal intensity changes in the LW are shown in Fig. 5 for  $\text{Mn}^{2+}$  infusion alone (filled square),  $\text{Mn}^{2+}$  infusion plus dobutamine (at 14.0 nmoles/min/g BW  $\text{Mn}^{2+}$  (open triangle)), and  $\text{Mn}^{2+}$  infusion plus diltiazem (at 3.3 nmoles/min/g BW  $\text{Mn}^{2+}$  (open circle)). Dobutamine increased the steady-state signal enhancement, and diltiazem decreased the steady-state signal enhancement significantly compared to control. The values of percentage signal enhancement with dobutamine and diltiazem are shown in Table 2 for all of the ROIs measured and at different  $\text{Mn}^{2+}$  infusion doses. The ROIs considered were the S, LV, CW, and L. At 14.0 nmoles/min/g BW infused  $\text{Mn}^{2+}$ , dobutamine increased the steady-state signal enhancement by 102% for both the S and LV compared

Table 1  
Steady-State Signal Enhancement From  $T_1$ -Weighted MRI Due to Infusion of  $\text{MnCl}_2$  at Various Concentrations

ROIs	Control			3.3 nmoles/min/g		
	Pre-Dob (n = 4)	Post-Dob (n = 3)	Enhance (%)	Pre-Mn (n = 3)	Post-Mn (n = 3)	Enhance (%)
Septum	103 ± 5	97 ± 7	0.1 ± 8.1	102 ± 3	145 ± 8 <sup>§</sup>	42.3 ± 5.8*
LV wall	101 ± 5	101 ± 10	0.7 ± 8.5	101 ± 2	149 ± 7 <sup>§</sup>	48.0 ± 9.1*
CW	104 ± 5	107 ± 14	6.1 ± 7.5	100 ± 4	103 ± 14	1.9 ± 10.4
Liver	108 ± 7	120 ± 28	11.9 ± 25.4	103 ± 4	173 ± 22 <sup>†</sup>	66.6 ± 14.2
HR	416 ± 39	513 ± 17	—	390 ± 52	386 ± 11	—
ROIs	7.0 nmoles/min/g			14.0 nmoles/min/g		
	Pre-Mn (n = 3)	Post-Mn (n = 3)	Enhance (%)	Pre-Mn (n = 6)	Post-Mn (n = 6)	Enhance (%)
Septum	101 ± 1	148 ± 13 <sup>§</sup>	46.4 ± 12.2*	102 ± 6	144 ± 13 <sup>§</sup>	41.1 ± 15.3*
LV wall	100 ± 2	155 ± 20 <sup>§</sup>	54.6 ± 22.1*	102 ± 9	149 ± 14 <sup>§</sup>	47.0 ± 17.5*
CW	100 ± 0	106 ± 5	6.0 ± 4.5	102 ± 7	122 ± 26	18.7 ± 17.3
Liver	101 ± 2	152 ± 25	50.3 ± 26.7	102 ± 5	142 ± 32	39.9 ± 32.6
HR	390 ± 25	395 ± 16	—	367 ± 50	385 ± 54	—

Heart rate (HR), interventricular septum (Septum), left ventricular free wall (LV Wall), chest wall (CW), pre-dobutamine (Pre-Dob), post-dobutamine (Post-Dob), pre-manganese infusion (Pre-Mn), and post-manganese infusion (Post-Mn). Values are expressed in mean ± SD as normalized percentage to initial images acquired at the start of each experiment. Statistics are done with ANOVA with Scheffe test between groups.

\* $P < 0.01$ , signal enhancement % compared to control; <sup>†</sup> $P < 0.05$ , Post- versus Pre-infusion; <sup>§</sup> $P < 0.01$ , Post- versus Pre-infusion.

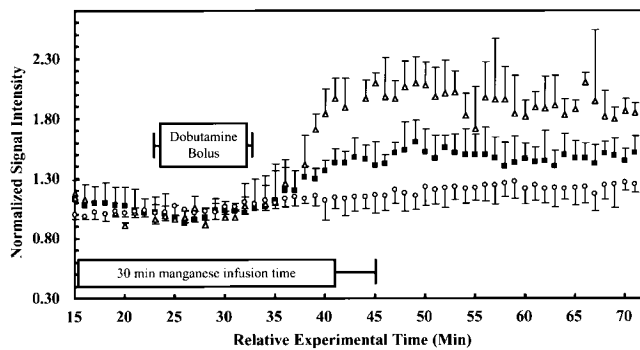


FIG. 5. Time course of  $T_1$ -weighted MRI signal intensity changes in the LW for manganese infusion alone (filled square), manganese infusion (14.0 nmoles/min/g BW) plus dobutamine ( $1.52 \pm 0.21 \mu\text{g/g}$  BW ip; open triangle), and manganese infusion (3.3 nmoles/min/g BW) plus diltiazem ( $0.017 \pm 0.002 \mu\text{g/min/g}$  BW; open circle). Each point represents the average pixel value taken from the LW ROI and normalized to the external reference and the average of images taken before any infusion. (Error bars = 1 SD.)

to  $\text{Mn}^{2+}$  infusion alone. Similar increases in signal enhancements were detected at 3.3 nmoles/min/g BW infused  $\text{Mn}^{2+}$  for dobutamine plus  $\text{Mn}^{2+}$  vs.  $\text{Mn}^{2+}$  alone. For diltiazem, the percentage signal enhancements were 13%, 20%, -4%, and 45% for the S, LV, CW, and L, respectively. There was a 69% and 59% signal intensity decrease for diltiazem plus  $\text{Mn}^{2+}$  compared to  $\text{Mn}^{2+}$  infusion alone for the S and LV wall, respectively.

In addition to the steady-state signal enhancements the rate of increase in signal due to  $\text{Mn}^{2+}$  infusion was analyzed. A rate constant describing the rise time for all the experiments was obtained from first-order exponential fitting to the normalized signal intensity starting from the

Table 3

Signal Rise Time Rate Constant for Left Ventricular Free Wall Due to Various Manganese Concentrations, and Inotropic Conditions

	Rise time rate constant ( $\cdot 10^{-2} \cdot \text{min}^{-1}$ )
Control (n = 4)	$1.40 \pm 1.40$
3.3 nmoles/min/g (n = 3)	$5.73 \pm 4.00$
7.0 nmoles/min/g (n = 3)	$12.21 \pm 1.00$
14.0 nmoles/min/g (n = 5)	$12.43 \pm 3.10$
14.0 nmoles/min/g + Dobutamine (n = 3)	$30.90 \pm 3.40$
3.3 nmoles/min/g + Diltiazem (n = 4)	$3.75 \pm 9.40$

Values are expressed in mean  $\pm$  SD.

time when the signal enhancement began. The rate constants obtained are shown in Table 3 for the LW for the various conditions. The rise time rate constant increased with increasing  $\text{Mn}^{2+}$  infusion dose and reached a plateau of  $\approx 12 \text{ min}^{-1}$  at 7.0 nmoles/min/g BW infused  $\text{Mn}^{2+}$  dose. With dobutamine the rate constant increased to  $\approx 31 \text{ min}^{-1}$ , and with diltiazem the rate constant decreased to  $\approx 4 \text{ min}^{-1}$ .

## DISCUSSION

$\text{Mn}^{2+}$  is paramagnetic and has been used to enhance MRI signal by the shortening of water  $T_1$ . Indeed  $\text{MnSO}_4$  was the first agent suggested for use as an MRI contrast agent by Lauterbur et al. (15). There have been numerous MRI studies that have measured the biodistribution of injected  $\text{Mn}^{2+}$  and  $\text{Mn}^{2+}$  chelates, such as  $\text{MnDPDP}$ , to further the use of  $\text{Mn}^{2+}$  as an MRI contrast agent (22–24). Recently, it has been demonstrated that  $\text{Mn}^{2+}$  can be used to enhance excitable cells in the brain as a

Table 2

Steady-State Signal Enhancement Increases or Decrease Due to Dobutamine or Diltiazem, Respectively

ROIs	14.0 nmoles/min/g			14.0 nmoles/min/g + dobutamine		
	Pre-Mn (n = 6)	Post-Mn (n = 6)	Enhance (%)	Pre-Mn (n = 4)	Post-Mn (n = 4)	Enhance (%)
Septum	$102 \pm 6$	$144 \pm 13^{\text{S}}$	$41.1 \pm 15.3$	$101 \pm 3$	$186 \pm 22^{\text{S}}$	$83.5 \pm 17.2^{+\dagger}$
LV wall	$102 \pm 9$	$149 \pm 14^{\text{S}}$	$47.0 \pm 17.5$	$101 \pm 2$	$197 \pm 17^{\text{S}}$	$94.8 \pm 16.4^{+\dagger}$
CW	$102 \pm 7$	$122 \pm 26$	$18.7 \pm 17.3$	$99 \pm 3$	$127 \pm 22$	$27.6 \pm 19.6^{\#\text{}}$
Liver	$102 \pm 5$	$142 \pm 32^{\dagger}$	$39.9 \pm 32.6$	$103 \pm 6$	$209 \pm 11^{\text{S}}$	$103.1 \pm 21.8^{\wedge\#}$
HR	$367 \pm 50$	$385 \pm 54$	—	$375 \pm 47$	$527 \pm 26$	—
ROIs	3.3 nmoles/min/g + dobutamine			3.3 nmoles/min/g + diltiazem		
	Pre-Mn (n = 2)	Post-Mn (n = 2)	Enhance (%)	Pre-Mn (n = 5)	Post-Mn (n = 5)	Enhance (%)
Septum	$101 \pm 1$	$173 \pm 32^{\text{S}}$	$82.9 \pm 16.9^{\wedge\dagger}$	$101 \pm 0$	$114 \pm 15$	$12.9 \pm 15.1^{\wedge}$
LV wall	$102 \pm 2$	$187 \pm 37^{\text{S}}$	$97.1 \pm 20.0^{\wedge\dagger}$	$101 \pm 2$	$121 \pm 12$	$19.5 \pm 11.4^{\wedge}$
CW	$100 \pm 1$	$102 \pm 3$	$62.4 \pm 19.1$	$101 \pm 2$	$97 \pm 10$	$-3.6 \pm 9.1$
Liver	$104 \pm 4$	$193 \pm 8^{\text{S}}$	$84.4 \pm 0.4$	$103 \pm 2$	$147 \pm 17^{\dagger}$	$43.6 \pm 15.0$
HR	$420 \pm 14$	$531 \pm 18$	—	$366 \pm 51$	$359 \pm 58$	—

Heart rate (HR), interventricular septum (Septum), left ventricular free wall (LV Wall), and chest wall (CW). Values are expressed in mean  $\pm$  SD as normalized percentage to initial images acquired at the start of each experiment. Statistics are done with ANOVA with Scheffe test between groups.

\* $P < 0.01$ , signal enhancement % compared to 120 mM  $\text{Mn}^{2+}$ ;  $\wedge P < 0.05$ , signal enhancement % compared to 120 mM  $\text{Mn}^{2+}$ ;  $\dagger P < 0.01$ , signal enhancement % compared to 30 mM + Diltiazem;  $\# P < 0.05$ , signal enhancement % compared to 30 mM + Diltiazem;  $\text{S} P < 0.01$ , Post- versus Pre-infusion;  $\dagger P < 0.05$ , Post- versus Pre-infusion.

technique to image regional brain activation by MRI (16). Several other reports have verified this use of  $Mn^{2+}$  as a functional brain contrast agent (25,26). These studies utilized the ability of  $Mn^{2+}$  to enter cells through voltage-gated channels. Since voltage-gated calcium channels are found in a wide range of tissues it might be possible to use  $Mn^{2+}$  to assess calcium influx by MRI. Calcium influx is a key step in generating force during cardiac contraction, and changes in inotropic state are known to affect cardiac calcium influx. Indeed, building on the work using  $Mn^{2+}$  to mark excitable cells in the brain, coupled with the fact that the FDA-approved agent MnDPDP releases  $Mn^{2+}$ , has prompted a number of groups to investigate the usefulness of  $Mn^{2+}$  as an MRI contrast agent to detect ischemic cardiac tissue (24).

The present work was performed to see if the time course of  $Mn^{2+}$  enhancement of the heart could be modulated by altering the inotropic state of the heart with dobutamine, which is known to increase calcium influx, and diltiazem, which is known to decrease calcium influx. The long-term goal is to determine whether  $Mn^{2+}$  can be used to assess calcium influx rates in the heart by MRI. Concentrations of  $MnCl_2$  were infused intravenously into mice, resulting in large signal enhancements without affecting left ventricular ejection fraction or heart rate, and the mice survived for at least 1 month after the MRI experiments. However,  $Mn^{2+}$  is known to be cardiotoxic at high doses (27). Indeed, it is the toxic properties of  $Mn^{2+}$  that have limited its development as an MRI contrast agent. However,  $Mn^{2+}$  is also an essential element for maintaining cell viability. With the increase in stability and sensitivity of MRI scanners it should be possible to use much lower doses of  $Mn^{2+}$  than used in early studies to determine the suitability of  $Mn^{2+}$  as an MRI contrast agent. Our results indicate that, at least in mice, subtoxic doses can cause significant enhancement of the heart without affecting left ventricular ejection fraction or heart rate after the MRI experiments. Since we relied on short TRs rather than the inversion recovery pulse sequence, the  $T_1$  weighting used was not optimal. The dynamic range of enhancement with an optimal pulse sequence may therefore increase by a factor of 2 with the same  $Mn^{2+}$  dose. Furthermore, the signal enhancements detected with our protocol were relatively large, indicating that lower doses of  $Mn^{2+}$  could be used.

With 30 min of  $Mn^{2+}$  infusion there was a dose-dependent increase in signal intensity in  $T_1$ -weighted MRI of the heart. The signal increased over the 30-min infusion of  $Mn^{2+}$  and then maintained a steady state for at least 30 min after the infusion. Considering that the half-life of  $Mn^{2+}$  in blood is approximately 3 min (28), the fact that the enhancement persists is consistent with the model that  $Mn^{2+}$  is accumulating intracellularly, as suggested previously (24). Furthermore, it has been observed that  $Mn^{2+}$  infusion into perfused heart and isolated cardiomyocytes will quench the fluorescence of intracellular fluorescence probes (29). Indeed,  $Mn^{2+}$  influx has been used to quench the signal from intracellular fluorescent calcium probes, and the quenching rate of these probes has been used as a quantitative index of calcium influx (29). In sheep and rat hearts, infusion of

$Mn^{2+}$  led to a large linebroadening of intracellular phosphorus-containing compounds as detected by  $^{31}P$  NMR (Koretsky, unpublished observation). How long the enhancement can last is an open question. In the brain, regional enhancement due to  $Mn^{2+}$  accumulation in active regions lasted at least 2 h (16). At longer times (12–36 h),  $Mn^{2+}$  has been shown to leave brain cells and follow appropriate neuronal pathways (17). This property makes  $Mn^{2+}$  useful as an MRI tract tracer.

By varying the calcium homeostasis state of the heart with dobutamine (positive inotropy from increased calcium influx) and diltiazem (negative inotropy from calcium channel blocker), the signal intensity enhancement increased and decreased for each case, respectively. There are several possible reasons for this. We favor the interpretation that the rate and extent of  $Mn^{2+}$  enhancement is proportional to changes in calcium influx. However, there are other possibilities. The signal intensity enhancement could have changed due to changes in the heart rate causing variations in the TR of the experiments. This was checked by varying the TR at extreme cases from 300–700 ms; the variations of the signal intensity due to varying TR was much smaller than the signal enhancement due to  $Mn^{2+}$  infusion (data not shown). Furthermore, the fact that the signal was stable for at least 30 min after  $Mn^{2+}$  infusion argues against heart rate fluctuations being responsible for the detected enhancements. Another possible complication that may affect the interpretation that  $Mn^{2+}$  is reporting on calcium influx is that dobutamine and diltiazem probably modified coronary flow and changed the availability of  $Mn^{2+}$  to the heart. There are several observations that argue against this possibility. First, the signal intensity increase plateaued by 3.3 nmoles/min/g BW and did not increase significantly up to 14.0 nmoles/min/g BW infused  $Mn^{2+}$  solution. Assuming coronary flow does not depend on  $Mn^{2+}$  concentration and this concentration limit of  $Mn^{2+}$  does not affect heart function, the fact that the signal intensity plateaued with large variations of  $Mn^{2+}$  concentration argues that the rate limiting step is accumulation of  $Mn^{2+}$ , not delivery of  $Mn^{2+}$ . Diltiazem is known to have a coronary vasodilatory effect, but the signal enhancement rate was slower and the steady-state signal enhancement was lower compared to the 3.3 nmoles/min/g BW  $Mn^{2+}$  infusion alone, suggesting that the enhancement is rate limited by accumulation, not by delivery.

Diltiazem decreased the steady-state enhancement and the rate of  $Mn^{2+}$  accumulation. Diltiazem is a calcium channel blocker, so this result is consistent with the model that  $Mn^{2+}$  is entering cells and its accumulation is limited by calcium entry pathways (28). Similarly, dobutamine increased the steady-state enhancement and increased the rate of signal increase. Dobutamine is known to increase calcium influx into the heart (20); this result is consistent with the model that  $Mn^{2+}$ -induced enhancement is limited by calcium entry pathways. The rate constant describing the rate of increase was very sensitive to the different agents used, suggesting that this will be a quantitative index related to cardiac calcium influx. Furthermore, an accurate rate constant could be obtained 5 min after start of cardiac enhancement, indicating that there will be useful

experimental protocols that infuse  $Mn^{2+}$  for much shorter times than the 30 min used here. There may be species differences in the amount of calcium and  $Mn^{2+}$  that enters the heart per beat. Indeed, the rodent heart may be less dependent on extracellular calcium than are those of larger mammals (30). This means that the dose used will probably be much lower in larger mammals than that used here for mice.

In conclusion,  $Mn^{2+}$  infusion in the mouse leads to significant signal enhancement in  $T_1$ -weighted MRI in the heart. At the doses used, no significant effects on cardiac function were detected, indicating that  $Mn^{2+}$  was below cardiotoxic levels. The MRI signal enhancement observed increases with the positive inotrope dobutamine, and decreases with the calcium channel blocker diltiazem. These results suggest that the rate of  $Mn^{2+}$  enhancement may be used to estimate relative calcium influx in the heart. Furthermore, the technique may be applicable to myocardial viability studies in which calcium channels have been altered due to low flow or ischemic conditions, as suggested by Brurok and coworkers (31). For the technique to develop and be applicable for clinical use, the infusion protocol must be further optimized to minimize the  $Mn^{2+}$  dose, with maximized signal enhancement, so as to eliminate any possibilities of cardiotoxic effects from  $Mn^{2+}$ . Finally, our ability to do these studies in the in vivo mouse with altered calcium homeostasis should make MEMRI useful for studying a variety of mouse models.

## ACKNOWLEDGMENTS

The authors thank K. Hendrich, M.T. Li, F. Kernec, Y.Q. Zhang, C. Du, and D. Williams for helpful discussions and assistance. We are especially grateful for the instruction on animal preparation techniques provided by our recently deceased colleague, Maryann Butowicz. This work was supported by NIH grants HL40354 to A.P. Koretsky and HL03826 to G. MacGowan, and the NINDS intramural research program (S. Landis, Scientific Director).

## REFERENCES

- van der Geest RJ, Reiber JH. Quantification in cardiac MRI. *J Magn Reson Imaging* 1999;10:602–608.
- Kroft LJ, de Roos A. Blood pool contrast agents for cardiovascular MR imaging. *J Magn Reson Imaging* 1999;10:395–403.
- Sakuma H, Kawada N, Takeda K, Higgins CB. MR measurement of coronary blood flow. *J Magn Reson Imaging* 1999;10:728–733.
- Chia YH, Wood ML, Leung WM, Plewes DB. Aorta wall motion monitoring by 1-d MRI of perpendicular diameters. *J Magn Reson Imaging* 1999;10:833–840.
- Spritzer C, Gamsu G, Sostman HD. Magnetic resonance imaging of the thorax: techniques, current applications, and future directions. *J Thorac Imaging* 1989;4:1–18.
- Zerhouni EA, Parish DM, Rogers WJ, Yang A, Shapiro EP. Human heart: tagging with MR imaging—a method for noninvasive assessment of myocardial motion. *Radiology* 1988;169:59–63.
- Schaefer S, Balaban RS. Cardiovascular magnetic resonance spectroscopy. Boston: Kluwer Academic Publishers; 1993. 230 p.
- Marban E, Kitakaze M, Koretsune Y, Yue DT, Chacko VP, Pike MM. Quantification of  $[Ca^{2+}]_i$  in perfused hearts. Critical evaluation of the 5F-BAPTA and nuclear magnetic resonance method as applied to the study of ischemia and reperfusion. *Circ Res* 1990;66:1255–1267.
- Li W-H, Fraser SE, Meade TJ. A calcium-sensitive magnetic resonance imaging contrast agent. *J Am Chem Soc* 1999;121:1413–1414.
- Hunter DR, Komai H, Haworth RA, Jackson MD, Berkoff HA. Comparison of  $Ca^{2+}$ ,  $Sr^{2+}$ , and  $Mn^{2+}$  fluxes in mitochondria of the perfused rat heart. *Circ Res* 1980;47:721–727.
- Narita K, Kawasaki F, Kita H. Mn and Mg influxes through Ca channels of motor nerve terminals are prevented by verapamil in frogs. *Brain Res* 1990;510:289–295.
- Shibuya I, Douglas WW. Indications from Mn-quenching of Fura-2 fluorescence in melanotrophs that dopamine and baclofen close Ca channels that are spontaneously open but not those opened by high  $[K^+]_o$ ; and that Cd preferentially blocks the latter. *Cell Calcium* 1993;14:33–44.
- Cory DA, Schwartzentruber DJ, Mock BH. Ingested manganese chloride as a contrast agent for magnetic resonance imaging. *Magn Reson Imaging* 1987;5:65–70.
- Mendonca-Dias MH, Gaggelli E, Lauterbur PC. Paramagnetic contrast agents in nuclear magnetic resonance medical imaging. *Semin Nucl Med* 1983;13:364–376.
- Lauterbur PC, Mendonca-Dias MH, Rudin AM. Augmentation of tissue water proton spin-lattice relaxation rates by in-vivo addition of paramagnetic ions. *Front Biol Energy* 1978;1:752.
- Lin YJ, Koretsky AP. Manganese ion enhances  $T_1$ -weighted MRI during brain activation: an approach to direct imaging of brain function. *Magn Reson Med* 1997;38:378–388.
- Pautler RG, Silva AC, Koretsky AP. In vivo neuronal tract tracing using manganese-enhanced magnetic resonance imaging. *Magn Reson Med* 1998;40:740–748.
- Slawson SE, Roman BB, Williams DS, Koretsky AP. Cardiac MRI of the normal and hypertrophied mouse heart. *Magn Reson Med* 1998;39:980–987.
- Ruff J, Wiesmann F, Hiller KH, Voll S, von Kienlin M, Bauer WR, Rommel E, Neubauer S, Haase A. Magnetic resonance microimaging for noninvasive quantification of myocardial function and mass in the mouse. *Magn Reson Med* 1998;40:43–48.
- Varro A, Papp JG. Classification of positive inotropic actions based on electrophysiologic characteristics: where should calcium sensitizers be placed? *J Cardiovasc Pharmacol* 1995;26:S32–S44.
- Nayler WG, Poole-Wilson P. Calcium antagonists: definition and mode of action. *Basic Res Cardiol* 1981;76:1–15.
- Ni Y, Petre C, Bosmans H, Miao Y, Grant D, Baert AL, Marchal G. Comparison of manganese biodistribution and MR contrast enhancement in rats after intravenous injection of MnDPDP and  $MnCl_2$ . *Acta Radiol* 1997;38:700–707.
- Brurok H, Schjott J, Berg K, Karlsson JO, Jynge P. Effects of MnDPDP, DPDP—, and  $MnCl_2$  on cardiac energy metabolism and manganese accumulation. An experimental study in the isolated perfused rat heart. *Invest Radiol* 1997;32:205–211.
- Saeed M, Higgins CB, Geschwind J, Wendland MF.  $T_1$ -relaxation kinetics of extracellular, intracellular and intravascular MR contrast agents in normal and acutely reperfused infarcted myocardium using echo-planar MR imaging. *Eur Radiol* 2000;10:310–318.
- Aoki I, Tanaka C, Ebisu T, Katsuta K, Fujikawa A, Umeda M, Fukunaga M, Watanabe Y, Someya Y, Fukuda K, Takegami T, Naruse S. Mismatch between the manganese ion influx and decreased apparent diffusion coefficient of water in the focal ischemia. In: Proceedings of the 8th Annual Meeting of ISMRM, Denver, 2000. p 2012.
- Duong TQ, Silva AC, Lee SP, Kim SG. Functional MRI of calcium-dependent synaptic activity: cross correlation with CBF and BOLD measurements. *Magn Reson Med* 2000;43:383–392.
- Brurok H, Schjott J, Berg K, Karlsson JO, Jynge P. Effects of manganese dipyridoxyl diphosphate, dipyridoxyl diphosphate—, and manganese chloride on cardiac function. An experimental study in the Langendorff perfused rat heart. *Invest Radiol* 1995;30:159–167.
- Mahoney JP, Small WJ. Studies on manganese. 3. The biological half-life of radiomanganese in man and factors which affect this half-life. *J Clin Invest* 1968;47:643–653.
- Du C, MacGowan GA, Farkas DL, Koretsky AP. Calibration of the calcium dissociation constant of Rhod-2 in the perfused mouse heart using manganese quenching. *Cell Calcium* 2001;29:217–227.
- Langer GA. Calcium and the heart. New York: Raven Press; 1990. p 199–268.
- Brurok H, Skoglund T, Berg K, Skarra S, Karlsson JO, Jynge P. Myocardial manganese elevation and proton relaxivity enhancement with manganese dipyridoxyl diphosphate. Ex vivo assessments in normally perfused and ischemic guinea pig hearts. *NMR Biomed* 1999;12:364–372.